European Journal of Medicinal Chemistry 46 (2011) 2722–2735

Contents lists available at ScienceDirect

European Journal of Medicinal Chemistry

journal homepage: http://www.elsevier.com/locate/ejmech

Original article

Curcumin analogues as possible anti-proliferative & anti-inflammatory agents☆

A.-M. Katsori [a], M. Chatzopoulou [a,1], K. Dimas [b,1], C. Kontogiorgis [c], A. Patsilinakos [d], T. Trangas [e], D. Hadjipavlou-Litina [a,*]

[a] Department of Pharmaceutical Chemistry, School of Pharmacy, Aristotle University of Thessaloniki, Thessaloniki 54124, Greece
[b] Department of Pharmacology, School of Medicine, University of Thessaly, Larissa, Greece
[c] Institute of Pharmaceutical Sciences, School of Biomedical and Health Services, King's College of London, London, UK
[d] Rome Center for Molecular Design, Dipartimento di Chimica e Tecnologie del Farmaco, University of Rome "Sapienza", Rome, Italy
[e] Department of Biological Applications and Technologies, University of Ioannina, Ioannina, Greece

ARTICLE INFO

Article history:
Received 21 January 2011
Received in revised form
21 March 2011
Accepted 29 March 2011
Available online 5 April 2011

Keywords:
Curcumin analogues
Lipoxygenase
Aldose reductase
Carrageenin
Anti-inflammatory activity
Anti-proliferative activity

ABSTRACT

A series of novel curcumin analogues has been designed, synthesized and tested *in vitro*/*in vivo* as potential multi-target agents. Their anti-proliferative and anti-inflammatory activities were studied. Compounds **1b** and **2b** were stronger inhibitors of soybean lipoxygenase (LOX) than curcumin. Analogue **1b** was also the most potent aldose reductase (ALR2) inhibitor. Two compounds, (**1a** and **1f**) exhibited *in vivo* anti-inflammatory activity comparable to that of indomethacin, whereas derivative **1i** exhibited even higher activity. The derivatives were also tested for their anti-proliferative activity using three different human cancer cell lines. Compounds **1a**, **1b**, **1d** and **2b** exhibited significant growth inhibitory activity as compared to curcumin, against all three cancer cell lines. Lipophilicity was determined as R_M values using RPTLC and theoretically. The results are discussed in terms of the structural characteristics of the compounds. Docking simulations were performed on LOX and ALR2 inhibitor **1b** and curcumin. Compound **1b** is well fitted in the active site of ALR2, binding to the ALR2 enzyme in a similar way to curcumin. Allosteric interactions may govern the LOX-inhibitor binding.

1. Introduction

In the past years, targeted therapies towards a specific molecular target, reducing toxic effects and damage of normal tissues, have been applied in the treatment of cancer. Despite the initial enthusiasm for the efficacy of these treatments, cancer patients often develop drug resistance due to the activation of alternative pathways. In the meanwhile, multi-target drug strategies have emerged as a therapeutic approach to treat diseases that stem from a combination of factors, leading to the final pathology, such as cancer [1–6]. Using this strategy, a single molecule hits multiple targets, which participate in pathways implicated to a given disease, leading to a more efficacious therapy, minimizing the emergence of resistance.

It is generally accepted that there is a close association between cancer and chronic inflammation [7–9]. Inflammation and carcinogenesis have been extensively studied at the molecular level, revealing potential novel targets for the treatment and chemoprevention of a number of different types of cancers [10,11]. Epidemiological studies have also shown that chronic inflammation preexists in some types of cancer and various inflammatory mediators like cytokines and chemokines, are present in tumour sites.

It is therefore evident that the use of multi-target ligands, that interact with multiple targets, could be valuable for the treatment of the above mentioned pathophysiological conditions [12]. It has already been proven for a number of commercially available non-steroidal anti-inflammatory drugs (NSAIDs) that they possess a combination of these properties. Namely, Aspirin® and other non-steroidal anti-inflammatory drugs may prevent cancer, through their action as cycloxygenase-2 (COX-2) inhibitors [13,14]. Furthermore, Zileuton (*Zyflo*®), a 5-lipoxygenase inhibitor, prevents lung tumorigenesis [15].

Curcumin or diferuloylmethane (Fig. 1) is a polyphenolic natural derivative, coloured yellow, isolated from the dried rhizome of the herb *Curcuma longa Linn* (Turmeric). Turmeric has been used as a dietary pigment, spice and in traditional medicine, in India and

☆ Part of these results has been presented at: 14th Panhellenic Pharmaceutical Congress, May 9–11, 2009, Athens, Greece and XXth International Symposium on Medicinal Chemistry, August 31–September 4, 2008, Vienna, Austria.

* Correspondence author. Tel.: +302310997627; fax: +302310997679.
E-mail address: hadjipav@pharm.auth.gr (D. Hadjipavlou-Litina).

[1] These authors contributed equally to this work.

0223-5234/$ – see front matter © 2011 Elsevier Masson SAS. All rights reserved.
doi:10.1016/j.ejmech.2011.03.060

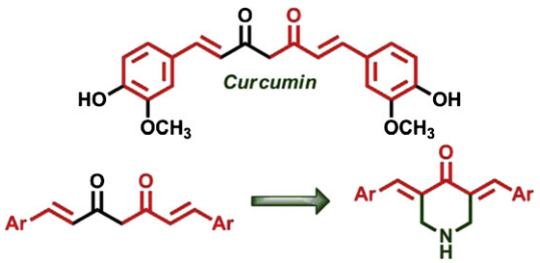

Fig. 1. Curcumin and curcumin analogues.

China, as an antiseptic, wound healing and anti-inflammatory agent. According to recent reviews, curcumin is a multi-target pleiotropic agent, exhibiting a broad range of biological activities. It interacts with multiple cellular targets implicated in cancer and inflammation [16–23]. Past and ongoing clinical trials have demonstrated that curcumin is safe at high doses and it seems to respond in various inflammatory and cancer-related diseases [16,23–27]. Although, its potential use as a therapeutic agent is severely affected by its low water solubility, rapid metabolism and poor bioavailability [20,28,29].

Thus, numerous approaches have been undertaken to synthesize new analogues and derivatives in order to enhance curcumin's bioavailability along with its anti-inflammatory or/and anticancer properties [20,30,31]. Recent reports have demonstrated that the β-diketone moiety of curcumin is a specific substrate for liver aldo-keto reductases. The presence of β-diketone may contribute to the rapid metabolism of curcumin *in vivo* [32].

In previous attempts to improve curcumin's poor pharmacokinetics a series of curcumin analogues containing a monocarbonyl moiety incorporated in a piperidone ring have been reported (Fig. 1). These analogues possess high anticancer activity [33–39]. Moreover, they induce apoptosis in human HL-60 promyelocytic leukaemia, HSC-2 squamous cell carcinoma and in human HepG2 liver cell lines [40], activate caspases −3, −8, and −9 [41], inhibit NF-κB [42], and stimulate fyn kinases [43], indicating that they can act upon a variety of cellular processes. All the above, support a multiplicity in biological targets, whereas no toxicity effects were observed in *in vivo* assays in mice [35,44]. Furthermore, evidence from a degradation degree and a pharmacokinetic *in vivo* study demonstrated that cycloexanone analogues have enhanced stability and activity compared to curcumin [45].

The presence of heteroaromatic cores is correlated with potent anti-proliferative and anti-inflammatory activities [33,45,46]. Thus, we decided to synthesize a series of curcumin analogues containing a variety of heterocyclic rings, (more specifically the indolyl, imidazolyl, thienyl) and the naphthyl ring in order to investigate their behaviour not only as proliferation inhibitors but as anti-inflammatory agents too. To evaluate the biological activity of the synthesized compounds, their ability to inhibit the inflammation-related enzymes Lipoxygenase (LOX) and Aldose Reductase (ALR2) was tested, as well as their anti-proliferative activity upon three different cancer cell lines (NCI-H460, MCF7 and SF268).

Compounds structurally similar to **1a** have marked affinities for thiols but not for amino or hydroxy groups [47a], which are found in nucleic acids. Thus, these compounds may be free from the mutagenicity/carcinogenicity, which is associated with a number of alkylating agents. The known "parent" molecule **1a** [44,47a] and the novel N-acryloyl derivative **2b** were synthesized and included in the biological study. Previous findings support the fact that N-acryloyl derivatives are more potent than N-acetyl or N-methyl derivatives [47b]. Since steric impedance to attack by thiols would be less in the case of **2b** than N-acetyl or N-methyl derivatives, it is conceivable that the N-acryloyl derivative would have greater potency.

2. Results and discussion

2.1. Chemistry

For the synthesis of the desired curcumin analogues **1a**–**i** two different synthetic approaches were followed: In *Method A*, a Claisen–Schmidt condensation was used [47] between the 4-piperidine hydrochloride monohydrate and the appropriate aryl aldehyde at a molar ratio 1:2, in acetic acid by passing through the mixture dry HCl gas. In *Method B*, an aldol condensation was recruited [48] between 4-piperidine hydrochloride monohydrate and the appropriate aryl aldehyde at a molar ratio 1:2 respectively, in an alcoholic solution of NaOH (10% *w*/*v*) (Scheme 1). All the synthesized analogues along with their physicochemical properties are presented in Table 1. Both methods were applied for the synthesis of compounds **1a**, **1c**, **1d**, **1h** and **1i**. For compounds **1a** and **1c** both methods led to the same products (they were identified spectrophotometrically and were found to be identical). Interestingly, attempts to synthesize **1d**, according to *Method B* resulted in the formation of a mixture of bis- and mono derivatives, whereas for **1h** and **1i** the same method produced the desired product more efficiently. Our attempt to synthesize the pyrrolyl analogue using both methods did not succeed. When *Method B* was used, a mixture of several different unidentified products was obtained. Using *Method A*, the reaction product was polymerized under acidic conditions.

Condensation of the free base **1b** with the acryloyl chloride led to the formation of **2b** (Scheme 2). All the synthesized compounds were characterized spectrophotometrically. Elemental analysis of C, H, and N, and melting points are given. Representative carbon nuclear magnetic resonance spectra were obtained. For compounds **1a**–**i**, the NH absorptions were not observed in the ^{1}H NMR spectra of the compounds, as it has already been refined by other researchers [40,41,43,44,47]. The X-ray crystallography studies of a number of previously synthesized analogues confirmed the isolation of *E*, *E* isomers [36,47], hence the assumption was made that the olefinic double bond possesses *E* stereochemistry.

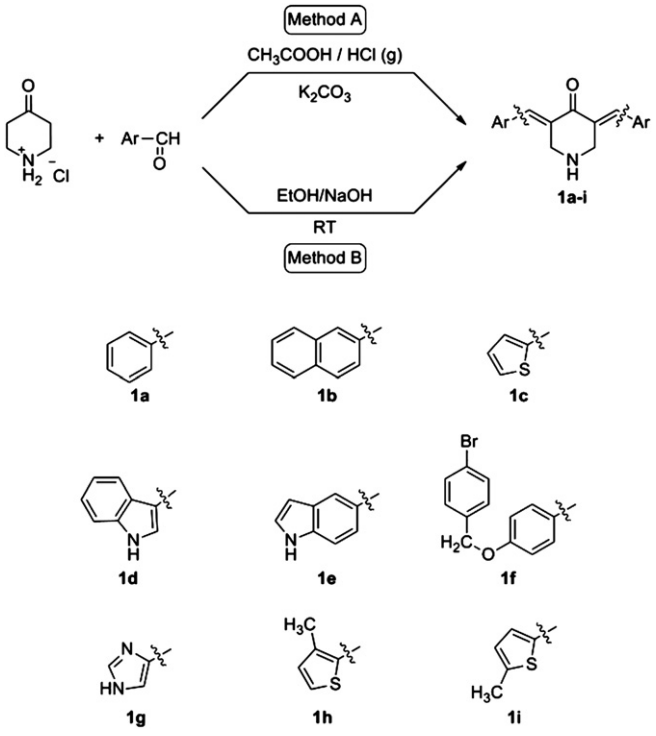

Scheme 1. General methods used for the synthesis of **1a**–**i** curcumin analogues.

Table 1
Lipophilicity values: theoretically calculated (clog *P*) and R_M values; theoretically calculated molecular refractivity values of Ar (MR-Ar) [72].

a/a	Ar	clog *P*	$R_M \pm SD$	MR-Ar
1a	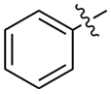	3.71	0.135 ± 0.00	2.59
1b	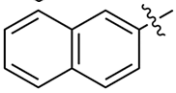	6.06	0.463 ± 0.00	4.27
1c	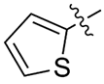	3.00	0.176 ± 0.00	2.40
1d	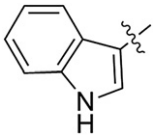	4.15	0.597 ± 0.08	3.70
1e	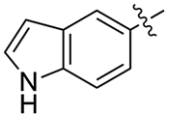	3.69	0.166 ± 0.025	3.70
1f	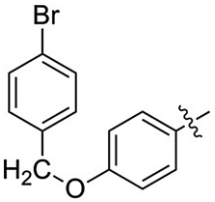	8.81	0.076 ± 0.0016	6.49
1g	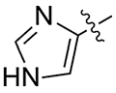	−0.63	−0.552 ± 0.042	1.80
1h	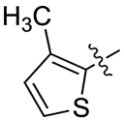	4.00	−0.030 ± 0.0017	1.86
1i	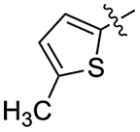	4.00	0.031 ± 0.0018	1.87
2b	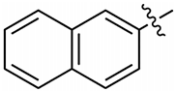	6.37	−0.050 ± 0.001	4.27

2.2. In vitro assays

2.2.1. In vitro inhibition of soybean lipoxygenase

Eicosanoids are oxygenated metabolites of arachidonic acid (AA) with broad implications in a variety of diseases. Upon appropriate stimulation of neutrophils, arachidonic acid is cleaved from membrane phospholipids and can be converted into leukotrienes (LTs) through 5-lipoxygenase (5-LOX). Leukotriene B4 (LTB4) is a potent mediator of inflammation, enhancing recruitment and activation of inflammatory cells. LTB4 generation is considered to be important in the pathogenesis of neutrophil-mediated inflammatory diseases [49] with a marked relation to the severity of

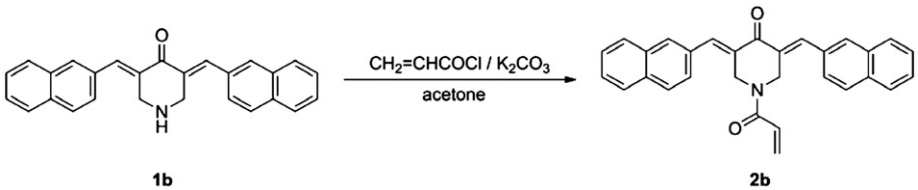

1b **2b**

Scheme 2. Synthesis of the N-acryloyl derivative **2b**.

Table 2
Soybean lipoxygenase (LOX) % at 100 μM and IC_{50} (μM) inhibitory activity; Aldose reductase (ALR2)% at 100 μM inhibitory activity data; Inhibition % of induced carrageenin rat paw oedema (CPE%) at 0.01 mmol/kg body weight.

Compound	LOX Inhibition ($C = 100$ μM)/IC_{50} (μM)	ALR2 Inhibition[a] ($C = 100$ μM)/IC_{50} (μM)	%CPE Inhibition[b]
1a	8%	49.0%	43.0*
1b	37 μM	70.6%	na[c]
1c	330 μM	45.5%	na[c]
1d	280 μM	27.8%	33.0*
1e	410 μM	na[c]	36.0*
1f	18%	na[c]	49.0*
1g	36%	na[c]	11.5*
1h	na[c]	56.0%	27.0*
1i	na[c]	na[c]	62.0*
2b	47 μM	37.5%	27.0*
Curcumin	38%	12.0%	
Sorbinil		0.25 μM[d]	
IMA[e]			47.0*

Each experiment was performed at least in triplicate and the standard deviation of absorbance was less than 10% of the mean.
* $p < 0.01$.
[a] $n < 3$.
[b] Statistical studies were done with student's *T*-test.
[c] No activity under the experimental conditions.
[d] Reported $IC_{50} = 0.25$ μM [78].
[e] Indomethacin.

cardiovascular diseases and cancer. Inhibitors of LOX have attracted attention initially as potential agents for the treatment of inflammatory and allergic diseases and certain types of cancer [12,50–54]. Recently in our laboratory, we have reported a series of aryl-acetic and aryl-hydroxamic acids acting as multi-target agents, possessing anti-LOX, anti-inflammatory and anticancer activities [55]. Curcumin has also been reported to inhibit 5-LOX activity both in *in vitro* and *in vivo* models [56–58].

LOXs contain a "non-heme" iron per molecule in the enzyme active site, as high-spin Fe^{2+} in the native state and the high-spin Fe^{3+} in the activated state. The four classes of direct 5-lipoxygenase inhibitors encompass: a) redox-active compounds keeping the active site iron in the ferrous state, thereby, uncoupling the catalytic cycle of the enzyme, b) iron ligand inhibitors, c) non-redox type inhibitors that compete arachidonic acid or lipid hydroperoxides for binding to 5-LOX and d) a novel class of inhibitors that may act in an allosteric manner [59].

Thus, we evaluated the ability of our analogues to inhibit soybean LOX by the UV absorbance based enzyme assay (Table 2) [60]. It is known that soybean lipoxygenase, which converts linoleic to 13-hydroperoxylinoleic acid, is inhibited by non-steroidal anti-inflammatory drugs (NSAIDs) in a qualitatively similar way to that of the rat mast cell lipoxygenase and may be used as a reliable screen for such activity [60].

Curcumin (BML-EI135) was used as a reference compound (inhibition 38% at 100 μM). Among the free bases, compound **1b** (IC_{50} 37 μM) was the most potent analogue followed by **1d**, **1c** and **1e**. Compounds **1a** and **1f** exhibited lower inhibition. Analogue **1g** at 100 μM seemed to be equipotent to curcumin whereas **1h** and **1i** do not present any inhibitory activity. Between the two indolyl-derivatives, the 3-substituted analogue (**1d**) was by far more potent compared to the 5-substituted analogue (**1e**). The acryloyl derivative **2b** presented high inhibitory activity (IC_{50} 47 μM) however, lower than that induced by the corresponding free base **1b**. Comparing the activities within the thienyl subgroup, only **1c** inhibited soybean LOX. It is also interesting that the imidazolyl-derivative **1g** was more potent than the phenyl analogue **1a**.Both compounds share the 4-piperidinone moiety with the two attached olefinic bonds. However, the replacement of phenyl by the imidazolyl ring increased the inhibitory activity. In previous studies, we found that the presence of a bromo-benzyloxy template diminishes LOX activity [61]. Herein, compound **1f**, containing this scaffold, did not confirm this finding.

Lipophilicity is referred as an important physicochemical property for LOX inhibitors [62] and in our case the higher lipophilicity value (clog *P*) supports the higher activity [clog *P* **2b** = 6.37, clog *P* **1b** = 6.06] (Table 1). The theoretically calculated clog *P* value of **1f** is too high to be realistic and thus, it was not taken under consideration in the discussion of the results.

Most of the LOX inhibitors are antioxidants or free radical scavengers [63]. In our case preliminary antioxidant studies did not demonstrate a significant antioxidant effect for the tested analogues (data not shown). The inhibitory activity of the compounds, which do not contain an easily oxidisable moiety, might be attributed mainly to their ability to attach to the active site of the enzyme or to act in an allosteric manner and to a lesser degree to their electron donating ability. It seems that replacement of H (N–H) by the acryloyl moiety (**2b**) does not significantly alter the inhibition pattern.

We further examined the possibility of compound **2b** acting as a prodrug of **1b**, though incubation of **2b**, under our experimental conditions, did not result in the production of **1b**.

2.2.2. *In vitro inhibition of aldose reductase*

Aldose reductase (ALR2) is the first enzyme of the polyol pathway and catalyzes the conversion of glucose to sorbitol. A number of studies, in the past years, demonstrated the implication of ALR2 in long-term diabetic complications. Nowadays, it has been found that ALR2 up-regulates a series of factors, involved in various pathological conditions [64]. Recently, Ramana et al. reviewed the implication of ALR2 in inflammatory pathologies, indicating the multiple roles of ALR2 inhibitors [65]. Curcumin has already been described as a specific ALR2 inhibitor [66,67]. It has also been published that curcumin analogues with structural similarities to the synthesized compounds, inhibit specifically rat lens ALR2 [68].

Our analogues were tested for their ability to inhibit purified rat lens ALR2 at 100 μM concentration. The human and rat sequences of ALR2 are characterized by 81% identity and 89% homology, while the proposed active sites of both enzymes are identical [69]. The assay, performed, was based on the spectrophotometric monitoring of NADPH oxidation from D, L-glyceraldehyde and is proven to be quite a reliable method [70]. Sorbinil was used as a positive control. Results are presented in Table 2 and are compared to curcumin (BML-EI135).

Under our experimental conditions compounds **1a**, **1b**, **1c**, **1d**, **1h**, **2b** were more potent inhibitors of ALR2 enzyme than curcumin. Among all the analogues **1b** seems to be the most potent followed by **1h**, **1a** and **1c**. The presence of the acryloyl group in **2b** reduces inhibitory activity. The 3-indolyl analogue **1d** inhibits ALR2, whereas the 5-indolyl **1e** had no effect under our experimental conditions. The substitution position of the methyl group on the thienyl rings influenced the biological response. Thus, analogue **1i** with a 5-CH_3 group did not present any activity, whereas the 3-CH_3 substituted analogue (**1h**) exhibited enhanced inhibition (56%) compared to the unsubstituted thienyl representative **1c**. The imidazolyl analogue **1g** also did not elicit any response. Perusal of % inhibition of ALR2 activity delineates the role of lipophilicity since the most potent analogue **1b** also exhibits the highest lipophilicity value (clog $P = 6.06$) compared to **1a**, **1b**, **1c**, **1d**, **1g** and **1h**.

2.2.3. *In vitro anti-proliferative activity*

The *in vitro* anti-proliferative activity studies were performed on three human cancer cell lines originating from solid tumours: NCI-H460 (Non small cell lung cancer), MCF7 (Breast Cancer) and SF268 (Central Nervous System, glioma) using the Sulforhodamine B assay [71]. The cells were preincubated for 24 h and subsequently

Table 3
In vitro anti-proliferative activity of all analogues against NCI-H460 (Non small cell lung cancer), MCF7 (Breast Cancer) and SF268 (Central Nervous System, glioma); Concentrations are in μM and represent the mean of three independent experiments each one run in triplicates. CV<15%.

Cell lines	Parameters	**1a**	**1b**	**1c**	**1d**	**1e**	**1f**	**1g**	**1h**	**1i**	**2b**	Curcumin
NCI-H460	GI_{50}	2.0	6.0	>100	3.5	>100	>100	>100	73.2	99.3	1.2	16.7
	TGI	6.1	24.5	>100	6.1	>100	>100	>100	>100	>100	5.5	50.1
	LC_{50}	10.3	98.3	>100	8.7	>100	>100	>100	>100	>100	9.8	83.4
	TI	5.2	16.4	nc[b]	2.4	nc[b]	nc[b]	nc[b]	1.4[a]	1.0[a]	8.1	5.0
MCF7	GI_{50}	0.8	6.8	>100	3.7	69.5	49.9	>100	63.0	80.7	1.4	4.7
	TGI	4.1	29.8	>100	6.0	>100	96.8	>100	>100	>100	5.3	8.3
	LC_{50}	9.0	97.5	>100	8.2	>100	>100	>100	>100	>100	9.2	67.2
	TI	11.6	14.3	nc[b]	2.2	1.4[a]	2.0[a]	nc[b]	1.6[a]	1.2[a]	6.6	14.2
SF268	GI_{50}	0.9	6.2	98.8	3.3	>100	>100	>100	53.8	65.2	0.6	5.1
	TGI	4.7	25.2	>100	5.7	>100	>100	>100	>100	>100	1.1	9.2
	LC_{50}	9.1	>100	>100	8.2	>100	>100	>100	>100	>100	8.3	61.0
	TI	10.0	16.0[a]	1.0[a]	2.5	nc[b]	nc[b]	nc[b]	1.9[a]	1.5[a]	13.8	11.9

GI_{50}: Growth Inhibitory Activity 50%; TGI: Total Growth Inhibitory activity; LC_{50}: Lethal Concentration 50%; TI: Therapeutic index (=LC_{50}/GI_{50}).
[a] The LC_{50} could not be determined as it was higher than 100 μM, the highest concentration of the compounds tested. Thus the TI was calculated by assuming $LC_{50} = 100$ μM.
[b] nc: not calculated.

incubated for 48 h with various concentrations of the analogues at 37 °C, 5% CO_2. The dose response parameters such as growth inhibition 50% (GI_{50}), total growth inhibition (TGI) and lethal concentration 50% (LC_{50}) were calculated. GI_{50} is the concentration of drug required to decrease the cell growth to 50%, compared with that of the untreated cell number. TGI is the concentration of drug required to totally inhibit cell growth. LC_{50} is the concentration of drug required to decrease the cell population by 50% of the initial cell number (Table 3, Figs. 2 and 3). Analogues **1g** and **1c** found to be inactive up to 100 μM, the highest concentration tested against all three cell lines used and the **1e** and **1f** derivatives demonstrate a low growth inhibitory activity only against the MCF7 cell line. Among the thienyl subgroup, the methyl substituted derivatives **1h** and **1i** seemed to be more potent compared to **1c**, with **1h** having the lower GI_{50} value. It seems that increase of lipophilicity enhances the biological response. Among analogues **1a**–**i**, compounds **1a**, **1b**, **1d** exhibited significant growth inhibitory activity (below 10 μM) against all three cell lines, under the experimental conditions used. The most active analogue, within series **1**, was found to be **1a**, exhibiting a GI_{50} close to 1 μM, against all cell lines. Compound **1d** exhibited lower inhibitory activity (higher GI_{50} value) than curcumin in all three cell lines. No differences in cytotoxic activity were detected when **1d** was compared to analogue **1a**, as this is reflected by the LC_{50} values. Therefore the 3-indolyl group seems to play a key role in the growth inhibitory activity of the analogues. This assumption is supported by the observation that the 3-indolyl-substitution (**1d**) resulted in complete inactivation. On the contrary the 5-indolyl analogue (**1e**) had no activity, revealing the detrimental role of the indolyl moiety ring 3/5 attachment. The analogue **1b** exhibited a significant growth inhibitory activity higher than that of curcumin in NCI-H460 cell line. However, this compound demonstrated as well, a much lower cytotoxic activity (LC_{50} close to 100 μM). Thus, considering the ratio of LC_{50}/GI_{50} as a Therapeutic Index (TI), compound **1b** presented the best TI among the most active analogues, including curcumin (Table 3). When an acryloyl group was further added to the **1b**, the resulting analogue **2b** showed increased both inhibitory and cytotoxic activities (Table 3). These data are in accordance to previous reports [47]. A detrimental contribution of lipophilicity is also shown in this case, since analogue **2b** possesses higher clog *P* than **1b** (Table 1).

Altogether the results from the preliminary screen suggest that **1a**, **1b**, **1d** and **2b** analogues, exhibit significant growth inhibitory activity against solid tumour derived cell lines. The observed GI_{50} values for these four derivatives upon the NCI-H460, MCF7 and SF268 cancer cell lines, reveal that the anti-proliferative activity within analogues **1a**–**i** is inversely correlated with the size of the aryl substituents, expressed as molar refractivity MR-Ar values (molar refractivity depends on volume and polarisability) (Table 1). The results suggest that steric hindrance plays an important role [MR-Ar-**1a** 2.586 < MR-Ar-**1d** 3.703 < MR-Ar-**1b** 4.274] [72]. The fact that at least one of the analogues synthesized in this work (**1a**) has already been reported to possess significant anti-leukaemic activity [47] strengthens further the notion that these compounds may be promising anticancer agents and need to be more thoroughly investigated. The presence of a naphthyl or of a 3-indolyl group appears to be critical in terms of structure activity relations.

2.3. *In vivo* anti-inflammatory activity

In *in vivo* acute toxicity experiments, the examined compounds did not cause toxic effects in doses up to 0.2 mmol/kg body weight. Ulcerogenicity was not observed. Compounds were tested for their anti-inflammatory activity *in vivo* (dose *intraperitoneally* 0.01 mmol/kg body weight). The *in vivo* anti-inflammatory effects of the tested compounds were assessed by using the functional model of carrageenin-induced rat paw oedema (CPE) [73] and are presented in Table 2, as percent inhibition of carrageenin-induced rat paw oedema.

After 3.5 h, compound **1g** provided very low protection (11.5%) against carrageenin-induced paw oedema while the reference drug indomethacin (IMA) induced 47% protection at an equivalent dose. Compounds **1b** and **1c** did not inhibit carrageenin-induced rat paw oedema, whereas compound **1i** caused the highest inhibition among the tested compounds (62%) followed by the **1f** (49%). No difference was observed between the two indolyl analogues which showed to be equipotent. The side ring's attachment site did not seem to influence the biological response (**1d** and **1e**, 33% and 36%). Concerning the thienyl derivatives it is interesting that the potency increased when a methyl group was attached to the 5-position of the ring (**1i**). Reduced anti-inflammatory activity was observed for the **1h** (3-substituted) and the activity was diminished for the unsubstituted derivative **1c**. Herein the role of lipophilicity is marginal (**1i** > **1c**, **1h** > **1c**). The "parent" derivative **1a** produces satisfactory inhibition of the carrageenin induced rat paw oedema (43%). As shown in Table 2, analogue **1b** appeared inactive, whereas the acryloyl **2b** possessed anti-inflammatory properties. This behaviour might be attributed to the conformation imposed by the addition of the acryloyl group in structure **1b**.

2.4. Physicochemical studies

The variations in the *in vivo* anti-inflammatory activity of the tested compounds could partially be attributed to differences in their physicochemical properties, which determine their

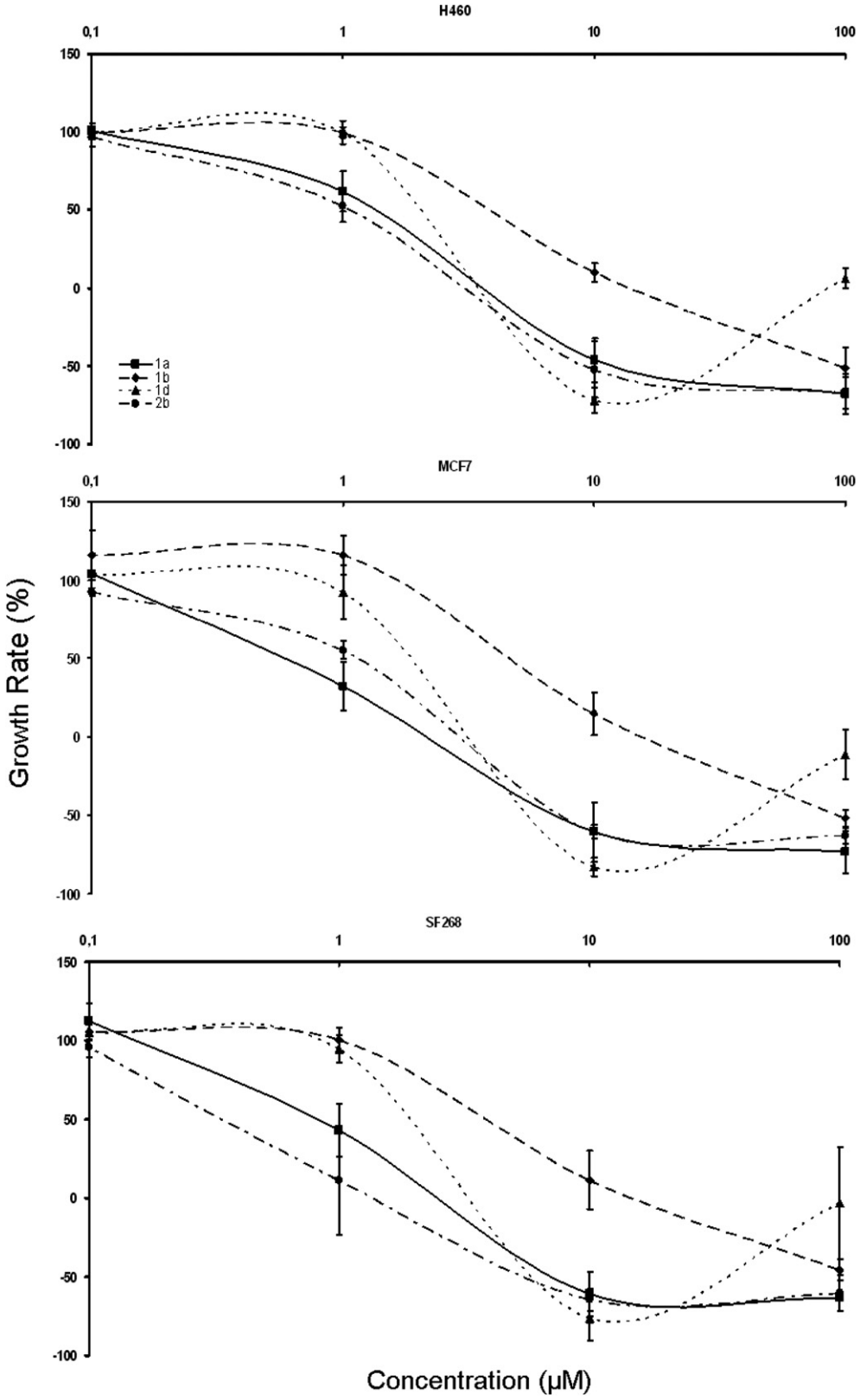

Fig. 2. Percent growth rates of the three cell lines H460, MCF7 and SF268 after treatment with various concentrations of the four analogues **1a**, **1b**, **1d** and **2b** for 48 h. The curves were generated using the SRB assay. Each point represents the mean of three independent experiments, each one run in triplicates ± SD.

distribution in the body and their ability to cross membranes and enter cells [74,75]. Lipophilicity is a significant physicochemical property, determining distribution, bioavailability, metabolic activity and elimination. Thus, this parameter was experimentally determined for each compound as R_M value. The Reverse Phase Thin-Layer Chromatography (RPTLC) method was used [61] and R_M values were compared to the corresponding theoretically calculated clog *P* values in n-octanol [72]. Even though, this is considered to be

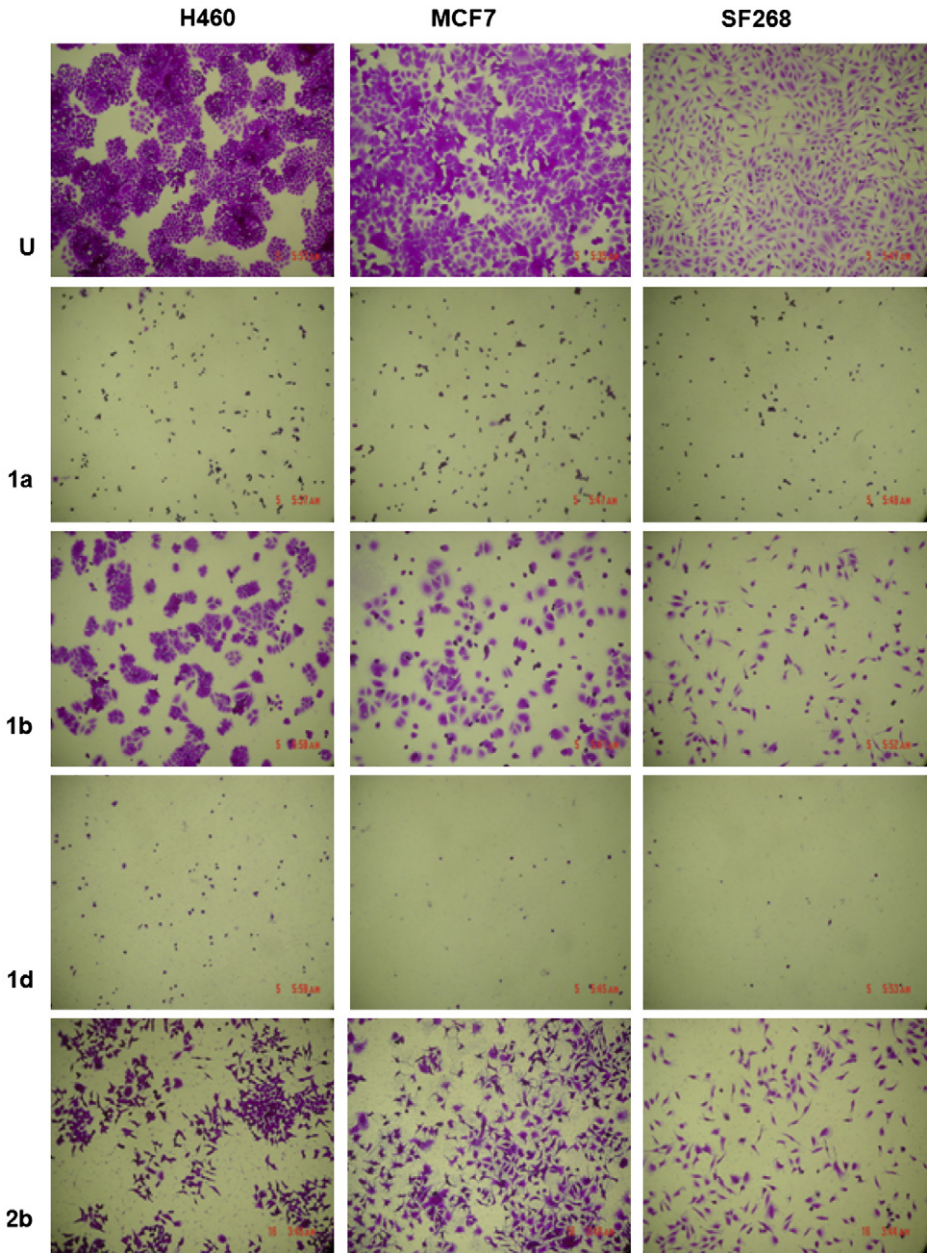

Fig. 3. Morphology of untreated cells from the three cell lines used for the *in vitro* screening (Ut) and after treatment with a concentration of 10 μM of the analogues **1a**, **1b**, **1d** and **2b** for 48 h. At the end of the 48 h incubation time cells were fixed with TCA and stained with SRB. DMSO which used as a vehicle solvent did not exhibit any activity (not shown). Pictures are from one representative out of three independent experiments. Magnification 10× at a Zeiss Axiovert 200M inverted microscope.

a reliable, fast and convenient method for expressing lipophilicity, our results (Table 1) indicate that R_M values could not be used as a successful relative measure of the overall lipophilic/hydrophilic balance of these molecules. This can be attributed to the different nature of the hydrophilic and lipophilic phases in the two systems and to the presence of basic nitrogen atoms in the examined compounds, which could disturb the absorption/desorption process.

2.5. Molecular docking studies

2.5.1. Docking studies on aldose reductase

In terms of analyzing the interactions of the synthesized analogues in the active site of ALR2, docking simulations were performed. The human aldose reductase holoenzyme, complexed with the inhibitor IDD 594 (PDB entry 1US0), was chosen [76], since it was determined at the highest resolution (0.66 Å) among all the available structures. Docking was carried out using the automated docking program Autodock Vina [77].

The structure of ALR2 active site has been extensively analyzed by both crystallographic and modelling studies. It has proved to be highly hydrophobic in nature and is formed by aromatic residues (Trp20, Tyr48, Trp79, Trp111, Phe121, Phe122 and Trp219), apolar residues (Val47, Pro218, Leu300 and Leu301), and polar residues (Gln49, Cys298 and His110). The nicotinamide ring of $NADP^+$ is centered in the cavity and the three possible proton donors responsible for catalysis are Tyr48, His110 and Trp111 all composing the anionic binding pocket [64,78].

In Fig. 4A the alignment of our analogue **1b** with both the inhibitor of ALR2 and curcumin is clearly shown, in the active site of

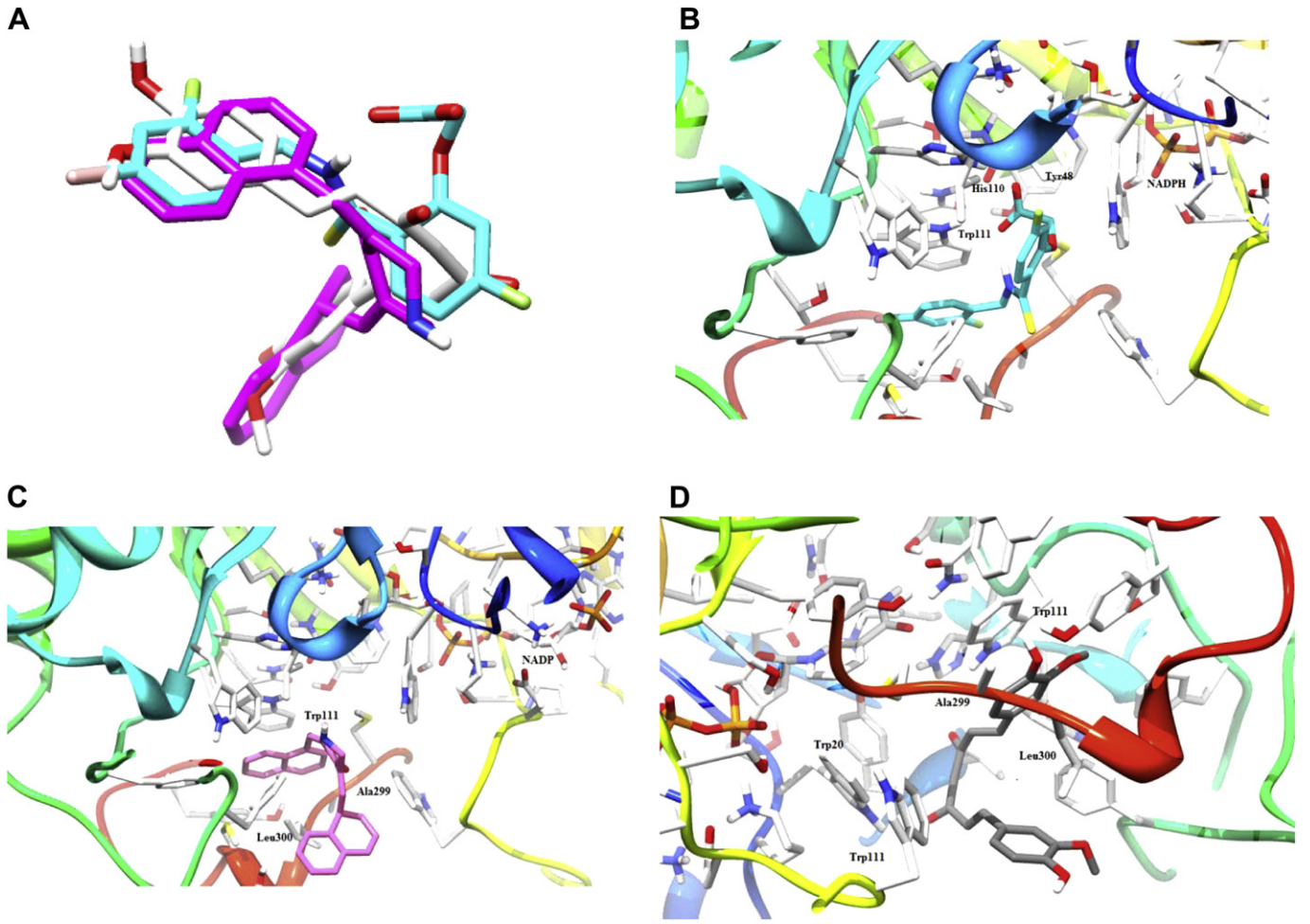

Fig. 4. Docked poses of (A) alignment of ligand IDD 594 (cyano), curcumin (white) and **1b** (purple), (B) inhibitor IDD 594 in the active center of ALR2, (cyano) (C) curcumin (grey) and (D) analogue **1b** (purple) in the ALR2 binding site. (for interpretation of the references to colour in this figure legend, the reader is referred to the web version of this article.)

ALR2. In the catalytic site of ALR2 the interactions of the inhibitor IDD 594 are mostly polar (Fig. 4B). IDD 594 binds to the active site of ALR2 with the acidic function forming hydrogen bonds with Tyr48, His110 and Trp111, which are the three key residues in the binding site [79,80]. Additional strong electrostatic interactions with $NADP^{+}$ occur. The obtained docking results are in accordance with docking results already reported [76,81].

The best binding modes of the most active analogue **1b** and curcumin are presented in Fig. 4C and D. Compound **1b** exhibits binding energy slightly lower (−13.2 kcal/mol) than the selective inhibitor IDD 594 (−9.7 kcal/mol). Curcumin presents even higher binding energy (−8.4 kcal/com). These results seem to be in accordance with our biological data (Table 2).

Previous molecular docking studies with both keto and enol forms of curcumin revealed similar results with both tautomers [67]. Thus, for simplicity, we present our molecular docking data with the keto form of curcumin. The carbonyl group strongly interacts via hydrogen bonds with Trp20. Hydrogen bonds are also observed between one of the methoxy groups and Leu300 in the active site of the protein.

Analogue **1b** is well fitted in the active site of ALR2. Compared to the other two compounds, it creates different type of interactions with amino acids of the active site. No hydrogen bonding is observed in the case of analogue **1b**. Lipophilicity seems to play crucial role in **1b** inhibitory activity. The naphthyl groups are properly oriented to the more lipophilic areas of the ALR2 binding site whereas hydrophobic bonds are created with Trp111, Leu300 and Ala299.

2.5.2. Docking studies on soybean lipoxygenase

The lack of structural data for human LOX, lead us to model human LOX using soybean enzyme because of its availability and highly characterized structure [82]. The possible mechanism of action, as well as the differences in activity of our analogues toward soybean lipoxygenase could be explained by docking calculations. In our lab, we have a long experience in LOX inhibitors. We have recently presented a study of new LOX inhibitors, performing docking simulations on the most active compound to get some clues on the nature and type of interactions governing the inhibitor binding [83].

For the docking studies of lipoxygenase we have used the 1IK3 and 1RRH (soybean lipoxygenase) available from the Protein Data Bank (PDB) with a resolution of 2 Å [84]. We used the 1RRH from PDB with Fe^{+3} running blind docking. Two soybean lipoxygenase models were derived from 1RRH. One with a ligand taken from 1IK3 (ligand ID: 9OH) for the docking studies into the catalytic cavity and another one without any ligand in the catalytic cavity for the blind docking simulation. The metal center in both models has been considered as a cation, with charge $q = +3$ and no bond restraint was applied between the iron and the ligands. Lennard–Jones parameters for Fe(III) force field can be resumed as: $\sigma_{vdw} = 2.138157$ e−01 nm, $\varepsilon_{vdw} = 2.092$ e−1 kJ/mol. The validation

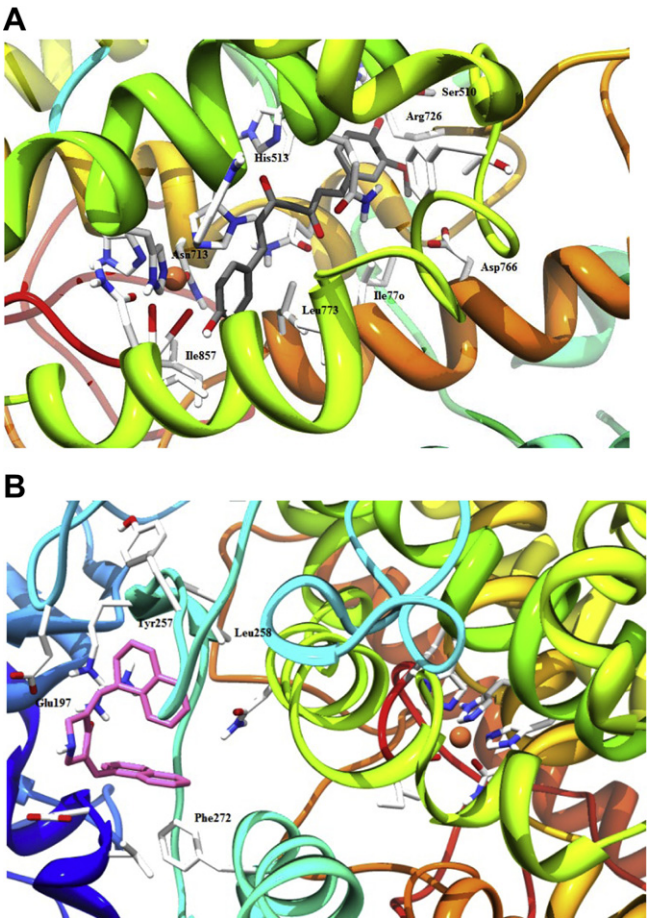

Fig. 5. Docked poses of (A) curcumin (dark grey) and (B) compound **1b** (purple) in the soybean lipoxygenase binding site. Side-chains of relevant binding site residues are rendered as ball and stick models. The iron ion is rendered as an orange sphere. (for interpretation of the references to colour in this figure legend, the reader is referred to the web version of this article.)

of our docking study was made with the ligands crystallized in the protein complexed to 1IK3, where our docking results were in good agreement with the structure of the molecules in the active site of the protein.

The docking orientations of the compounds are presented in Fig. 5. It is important to mention that analogue **1b** exhibits lower binding energy (−9.2 kcal/mol) to the protein than the reference compound curcumin. However, it was impossible for **1b** to get into the cavity, where curcumin was freely inserted (binding energy: −8.7 kcal/mol). The docking study suggests that the biological response of the examined compounds could be explained by the proper geometry of the predicted conformations at the active site.

In this docking approach it seems that curcumin creates significant interaction with many amino acids in the inner part of the cavity, near to the iron ion, forming hydrogen bonds with the amino acids of the cavity. The carboxylic group forms hydrogen bonding with His513 whereas one of the hydroxyl groups interacts with Arg726 in the lipoxygenase cavity. Significant bonds are observed between curcumin and the following amino acids: Ser510, Asn713, Asp766, Ile770, Leu773 and Ile857 (Fig. 5A).

As it is shown in Fig. 5B, analogue **1b** is well fitted in another area of the protein and not to the central cavity of LOX. Probable reason for this could be the bulk of naphthyl groups. π-interactions are developed among analogue **1b** and amino acids: Glu197, Trp257, Leu258, Gly265 and Phe272. The enzyme-inhibitor complex is stabilized by hydrophobic interactions between the aromatic moieties. From the above, the possibility of an allosteric effect might be considered. Furthermore, blockage of the cavity entrance might disturb the access to the catalytic site. The latter merits further investigation, since analogue **1b** could be a lead for the design of allosteric lipoxygenase inhibitors.

3. Conclusion

This study has demonstrated that curcumin analogues bearing a variety of heterocyclic substituents in the aromatic part combine anti-inflammatory and anti-proliferative activity. Some of our analogues proved to be more potent *in vitro* inhibitors of soybean lipoxygenase and aldose reductase (ALR2) enzymes than curcumin. The highest activity was exhibited by the naphthyl analogue **1b** in both assays. Compounds **1a**, **1b**, **1d** exhibited significant growth inhibitory activity (below 10 μM) against all three cancer cell lines. When an acryloyl group was further inserted to **1b**, the resulting analogue **2b** showed higher inhibitory activity whereas the anti-inflammatory activity was not enhanced. Compound **1i** presented a promising anti-inflammatory profile with high anti-oedematous activity, causing the highest inhibition of carrageenin induced paw oedema, among the tested compounds. The influence of lipophilicity is well documented. Lipophilicity correlated with the biological activity of the compounds. Furthermore, the presence of a naphthyl, or of a 3-indolyl group was critical for their effectiveness.

Molecular docking studies were carried out on the active compound **1b**. Modelling studies were found to be in accordance with our experimental biological results. The lipophilic analogue **1b** was well fitted into the active site of ALR2 enzyme, developing hydrophobic interactions. In the case of LOX enzyme the inhibitory activity of our analogue **1b** might be attributed to its ability to act in an allosteric way.

However, further investigation is needed in order to gain insight into the mechanism of action of the examined compounds. Some of the synthesized compounds might constitute initial leads for the design of new more potent multi-target therapeutic agents.

4. Experimental

4.1. General

All starting materials and solvents were obtained from commercial sources and used without further purification. Melting points were determined in open glass capillaries using a Mel-TempII apparatus (Lab. Devices, Holliston, MA, USA). UV–vis spectra were obtained on a Hitachi U-2001 spectrophotometer and on a Shimadzu UV-1700 PharmSpec (UVprobe Ver. 2.21). Infrared spectra (film as Nujol mulls or KBr) were recorded with a Shimadzu FT IR-8101 M and with a Perkin–Elmer FT-IR System BX. The ^{1}H NMR spectra were recorded at 300 MHz on a Bruker AM 300 spectrometer (Bruker Analytische Messtechnik GmbH, Rheinstetten, Germany) in $CDCl_3$ or DMSO using tetramethylsilane (TMS) as an internal standard, unless otherwise stated. ^{13}C NMR spectra were obtained at 75.5 MHz on a Bruker AM 300 spectrometer in $CDCl_3$ or DMSO solutions with tetramethylsilane as internal reference unless otherwise stated. MS (ESI) on a Shimadzu LC-MS 2010 EV. Elemental analyses were obtained in an acceptable range (±0.4%) in a Perkin–Elmer 240 B CHN analyzer (The Perkin–Elmer Corporation Ltd). Reactions were monitored by thin-layer chromatography (TLC) by Fluka, on aluminium cards precoated with 0.2 mm of silica gel and fluorescent indicator. For RPTLC silica gel Merck F_{254} plates were used.

For the biological assays soybean lipoxygenase, linoleic acid sodium salt NADPH, D-L-glyceraldehyde and indomethacin were

obtained from Sigma–Aldrich Corporation and carrageenin, type K, was commercially available. Curcumin (BML-EI135) was obtained from Biomol (Enzo Life Science) and Sorbinil from Pfizer, Inc. The cell lines NCI-H460 (Non small cell lung cancer), MCF7 (Breast Cancer) and SF268 (Central Nervous System, glioma) were obtained from the National Cancer Institute, NIH (Bethesda, MD, USA). Trichloro acetic acid (TCA), sulphorhodamine B (SRB) acetic acid, DMSO and trizma base were purchased from Sigma–Aldrich (St. Louis, MO, USA). All cell culture reagents were purchased from Euroclone Life Sciences Division (Milano, Italy). Microscopy analysis was performed with Axiovert 200M, Carl Zeiss, Gottingen, Germany equipped with a Sony digital camera. For the *in vivo* experiments, male and female Fischer-344 rats were used.

4.2. Synthesis

4.2.1. Synthesis of analogues **1a–i**

Two different methods were used for the synthesis of the compounds.

General Method A [44,47a]

A Claisen–Schmidt condensation was performed between 4-piperidine hydrochloride monohydrate and the appropriate aryl aldehyde at a molar ratio 1:2 in acetic acid. Dry hydrogen chloride was passed through the mixture for at least 1 h. After stirring at room temperature, the end of the reaction was monitored by TLC. The precipitate was then collected and added to a mixture of saturated aqueous potassium carbonate solution (25% *w*/*v*, 25 mL) and acetone (25 ml). The resultant mixture was stirred for 0.5 h. The free base is collected, washed with water (50 mL) and recrystallized from 95% aqueous ethanol. In the case where no precipitate was formed after the water dropping, extraction with 3 × 50 ml chloroform was performed and the organic base was collected and dried over K_2CO_3.

General Method B [48]

An aldol condensation between 4-piperidine hydrochloride monohydrate and the appropriate aryl aldehyde was performed at a molar ratio 1:2 respectively, in alcoholic NaOH (10% *w*/*v*). The solution was stirred at room temperature. The progress of the reaction was monitored using TLC. The separated solid was filtered, washed with water and recrystallized from the 95% aqueous ethanol.

4.2.1.1. 3,5-Dibenzylidenepiperidin-4-one (**1a**) [44,47a]

4.2.1.2. 3,5-Bis(naphthalen-1-ylmethylene)piperidin-4-one (**1b**).

Method A: 70% yield, yellow solid, m.p. 182–185 °C. R_f (8.5 benz:1.5 MeOH) 0.7. UV (ethanol absolute) λ_{max}: 270, 354 ε_{max}: 16580, 12390. IR (Nujol, cm^{-1}): 1660, 3400. ^1H NMR (DMSO-d_6) δ: 4.36–4.43 (s, 4H), 7.33 (d, 1H, *J* 6 Hz), 7.48 (d, 1H, *J* 8.1 Hz), 7.50–7.59 (m, 6H), 7.61–7.79 (m, 2H), 7.83–7.99 (m, 6H) ppm. The NH absorption of piperidone were not observed in the ^1H NMR spectra of the compounds as it has already been refined by other researchers [47a]. ^{13}C NMR (DMSO-d_6) δ: 40, 42.3, 103.8, 117.7, 122, 123, 124.3, 126, 129, 129.4, 130.2, 132, 134, 136, 138, 141.5, 142, 143, 144, 146, 147.6, 148, 152.3, 155, 157, 160, 179 ppm. LC-MS *m*/*z:* 376 $[M + H]^+$, 398 $[M + Na]^+$. Anal. calcd for $C_{27}H_{21}NO$: C 86.37, H 5.64, N 3.73. Found: C 86.20, H 5.70, N 3.76.

4.2.1.3. 3,5-Bis(thiophen-2-ylmethylene)piperidin-4-one (**1c**) [85]

4.2.1.4. 3,5-Bis((1H-indol-3-yl)methylene)piperidin-4-one (**1d**).

Method A: 10% yield, orange solid, m.p. 255 °C decomposes. R_f as hydrochloride salt (8.5 benz:1.5 MeOH) 0.2. UV as hydrochloride salt (ethanol absolute) λ_{max}: 260, 280, 453 ε_{max}: 14170, 13530, 29980. IR as hydrochloride salt (KBr, cm^{-1}): 1650, 3400. ^1H NMR as hydrochloride salt (DMSO-d_6) δ: 4.46 (s, 4H), 7.20–7.29 (m, 4H), 7.49–7.54 (m, 4H), 7.82–7.84 (m, 2H), 11.87 (m, 2H) ppm. The NH absorption of piperidone were not observed in the ^1H NMR spectra of the compounds as it has already been refined by other researchers [47a]. ^{13}C NMR as hydrochloride salt (DMSO-d_6) δ: 45, 45.12, 110.8, 110.9, 111.2, 112.9, 117.7, 118, 119, 120.5, 120.8, 122, 122.8, 127.5, 128, 128.2, 136, 144, 146, 146.9, 153, 154.7, 158.2, 182.2 ppm. LC-MS *m*/*z:* 354 $[M + H]^+$, 352 $[M - H]^+$, 376 $[M + Na]^+$, 392 $[M + K]^+$. Anal. calcd for $C_{23}H_{19}N_3O$: C 78.16, H 5.42 N 11.89. Found: C 78.04, H 5.36 N 11.49.

4.2.1.5. 3,5-Bis((1H-indol-5-yl)methylene)piperidin-4-one (**1e**).

Method A: 82% yield, red solid, m.p. 120 °C decomposes. R_f (EtOH) 0.9. UV (ethanol absolute) λ_{max}: 254, 298 ε_{max}: 5380, 3520. IR (Nujol, cm^{-1}): 1670, 3200–3450. ^1H NMR (DMSO-d_6) δ: 4.36 (br, 4H), 7.95–7.96 (m, 6H), 8.03–8.20 (br, 6H), 10.26 (s, 2H) ppm. The NH absorption of piperidone were not observed in the ^1H NMR spectra of the compounds as it has already been refined by other researchers [47a]. LC-MS *m*/*z:* 354 $[M + H]^+$. Anal. calcd for $C_{23}H_{19}N_3O$: C 78.16, H 5.42 N 11.89. Found: C 78.18, H 5.18 N 11.49.

4.2.1.6. 3,5-Bis(4-(4-bromobenzyloxy)benzylidene)piperidin-4-one (**1f**).

Method A: 28% yield, yellow solid, m.p. 210–213 °C. R_f (8.5 benz:1.5 MeOH) 0.8. UV (ethanol absolute) λ_{max}: 351 ε_{max}: 7510. IR (Nujol, cm^{-1}): 1670, 3300. ^1H NMR (DMSO-d_6) δ: 4.14 (s, 4H), 5.06 (s, 4H), 6.97–7.00 (m, 4H), 7.17–7.54 (m, 12H), 7.76–7.80 (br, 2H) ppm. The NH absorption of piperidone were not observed in the ^1H NMR spectra of the compounds as it has already been refined by other researchers [47a]. ^{13}C NMR (DMSO-d_6) δ: 39.6, 39.9, 76.5, 77, 110.9, 111, 114, 115, 116, 119, 121, 123, 124, 126, 127, 129, 131, 133, 135, 136, 137, 138, 139.8, 141, 143, 146, 147, 149, 151, 155, 159, 161, 183.6 ppm. LC-MS *m*/*z:* 646 $[M + H]^+$. Anal. calcd for $C_{33}H_{27}Br_2NO_3$: C 61.41, H 4.22 N 2.17. Found: C 61.3, H 4.08 N 1.88.

4.2.1.7. 3,5-Bis((1H-imidazol-2-yl)methylene)piperidin-4-one hydrochloride (**1g**).

Method A: 92% yield, white solid, m.p. 215 °C. R_f (8.5 benz:1.5 MeOH) 0.4. UV (ethanol absolute) λ_{max}: 283 ε_{max}: 3940. IR (Nujol, cm^{-1}): 1660, 3180, 3300. ^1H NMR (DMSO-d_6) δ: 4.19–4.26 (s, 4H), 6.09 (br, 2H), 7.42–7.49 (m, 2H), 9.70–9.73 (m, 4H) ppm. The NH absorption of piperidone were not observed in the ^1H NMR spectra of the compounds as it has already been refined by other researchers [47a]. The same problem was faced for the $[H^+]$ of the hydrochloride. LC-MS *m*/*z:* 254 $[M + H]^+$. Anal. calcd for $C_{13}H_{14}ClN_5O$: C 53.52, H 4.84 N 24.01. Found: C 53.86, H 4.41 N 23.64.

4.2.1.8. 3,5-Bis((3-methylthiophen-2-yl)methylene)piperidin-4-one (**1h**).

Method B: 83.4% yield, yellow solid, m.p. 159–162 °C. R_f (8.5 benz:1.5 MeOH) 0.6. UV (ethanol absolute) λ_{max}: 261, 400 ε_{max}: 8540, 23700. IR (Nujol, cm^{-1}): 1645, 3300. ^1H NMR (DMSO-d_6) δ: 1.15–1.35 (br, 6H), 4.05 (s, 4H), 7.08–7.35 (m, 4H), 7.66–7.72 (m, 2H) ppm. The NH absorption of piperidone were not observed in the ^1H NMR spectra of the compounds as it has already been refined by other researchers [47a] LC-MS m/*z:* 316 $[M + H]^+$, 314 $[M - H]^+$. Anal. calcd for $C_{17}H_{17}NOS_2$: C 64.73, H 5.43 N 4.44. Found: C 64.84, H 5.32 N 4.16.

4.2.1.9. 3,5-Bis((5-methylthiophen-2-yl)methylene)piperidin-4-one (**1i**).

Method B: 44% yield, orange solid, m.p. 181–182 °C. R_f (8.5 benz:1.5 MeOH) 0.5. UV (ethanol absolute) λ_{max}: 265, 402 ε_{max}: 10440, 25520. IR (Nujol, cm^{-1}): 1650, 3300. ^1H NMR (DMSO-d_6) δ: 1.35–1.60 (br, 6H), 4.10 (s, 4H), 6.70–6.81 (br, 2H), 7.15–7.24 (m, 2H), 7.85 (s, 2H) ppm. The NH absorption of piperidone were not observed in the ^1H NMR spectra of the compounds as it has already been refined by other researchers [47a]. ^{13}C NMR (DMSO-d_6) δ: 22, 21.4, 45.1, 46, 108.7, 111.7, 126.6, 133.8, 136, 137, 138.1, 147.1, 147.8, 148, 152, 155.3, 183.5 ppm. LC-MS *m/z:* 316 $[M + H]^+$, 314 $[M - H]^+$. Anal. calcd for $C_{17}H_{17}NOS_2$: C 64.73, H 5.43 N 4.44. Found: C 64.38, H 5.07 N 4.12.

*4.2.2. Synthesis of the acryloyl derivative **2b** [47]*

Acryloylchloride (1.11 mmol) was added to a suspension of 3,5-bis(naphthalen-1-ylmethylene)piperidin-4-one (0.72 mmol) in acetone (4 mL) and a solution of potassium carbonate (3.70 mmol) in water (1.3 mL) which was cooled externally with an ice bath. After stirring at room temperature, the reaction was monitored by TLC. The mixture was collected and diluted with water-ice (50–50). The precipitate was collected, washed with water and dried.

*4.2.2.1. 1-Acryloyl-3,5-bis(naphthalen-1-ylmethylene)piperidin-4-one (**2b**)*

91% yield, yellowish solid, m.p. 163–168 °C. R_f (8.5 benz:1.5 MeOH) 0.7. UV (ethanol absolute) λ_{max}: 264, 534 ε_{max}: 18250, 14500. IR (Nujol, cm^{-1}): 1640, 1653. ^1H NMR ($CDCl_3$) δ: 4.08 (s, 2H), 4.65–4.82 (br, 2H), 5.30–5.35 (dd, 1H, *J* 15 Hz), 6.02–6.05 (m, 2H), 7.40–7.58 (m, 10H), 7.91–7.93 (m, 4H), 8.00–8.03 (m, 2H) ppm. ^{13}C NMR ($CDCl_3$) δ: 50.6, 52, 103.4, 104, 112.1, 122, 123, 125.2, 126, 127.1, 128.7, 129.4, 130, 132, 134, 136, 138, 141.5, 142, 143, 144, 146, 147.6, 148, 149, 152.3, 155, 156.6, 162.7, 187 ppm. LC-MS *m/z:* 452 $[M + Na]^+$. Anal. calcd for $C_{30}H_{23}NO_2$: C 83.50, H 5.84 N 3.25. Found: C 83.50, H 5.45 N 3.05.

5. Physicochemical studies

5.1. Determination of lipophilicity as R_M values [61]

Reversed phase TLC (RPTLC) was performed on silica gel plates impregnated with 55% (*v*/*v*) liquid paraffin in light petroleum ether. The mobile phase was a methanol/water mixture (77:23 *v*/*v*). The plates were developed in closed chromatography tanks saturated with the mobile phase at 24 °C. Spots were detected under UV light. R_M values were determined from the corresponding R_f values (from 10 individual measurements) using the equation $R_M = \log [(1/R_f) - 1]$.

5.2. Determination of physicochemical parameters (lipophilicity as clog P and molar refractivity of substituents as MR-Ar) [72]

Lipophilicity was theoretically calculated as clog *P* values in n-octanol-buffer by CLOGP Programe of Biobyte Corp. Molar refractivity (MR-Ar) of selected substituents was also theoretically calculated by CLOGP [72].

6. Biological experiments

6.1. In vitro assays

In the *in vitro* assays each experiment was performed at least in triplicate and the standard deviation of absorbance was less than 10% of the mean.

6.1.1. Soybean lipoxygenase (LOX) inhibition study in vitro [61]

In vitro study was evaluated as reported previously [61]. The tested compounds, dissolved in DMSO, were incubated at room temperature with sodium linoleate (0.1 mM) and 0.2 mL of enzyme solution ($1/9 \times 10^{-4}$, *w*/*v* in saline). The conversion of sodium linoleate to 13-hydroperoxylinoleic acid at 234 nm was recorded and compared with the appropriate standard inhibitor. NDGA was used as an appropriate standard.

6.1.2. Aldose reductase (ALR2) enzyme assay

The target compounds as well as curcumin were dissolved in 10% aqueous solution of DMSO. Lenses were quickly removed from Fischer-344 rats of both sexes following euthanasia. The experiments conform to the law for the protection of experimental animals (Republic of Greece) and are registered at the Veterinary Administration of the Republic of Greece. ALR2 from rat lens was partially purified according to the reported procedure [78] as follows: lenses were quickly removed from rats following euthanasia and stored at −20 °C until used. The lenses were homogenized in 5 vol of cold distilled water. The homogenate was centrifuged at 10000 g at 0–4 °C for 15 min. The supernatant was precipitated with saturated ammonium sulphate at 40% salt saturation and this solution was centrifuged at 10000 g at 0–4 °C for 15 min. The latter supernatant was either used directly or stored for maximum 24 h at −80 °C.

ALR2 activity was assayed spectrophotometrically by determining NADPH consumption at 340 nm. In order to determine ALR2 inhibitory activity D, L-glyceraldehyde was used as a substrate. The target compounds were tested at the concentration of 100 μM.

6.1.3. Cell cultures

The cell lines were adapted to propagate in RPMI 1640 medium supplemented with 5% heat-inactivated foetal calf serum, 2 mM L-glutamine and antibiotics. The cultures were grown in a humidified 37 °C-incubator with 5% CO_2 atmosphere.

6.1.3.1. In vitro anti-proliferative activity [71]. Cell viability was assessed at the beginning of each experiment by the trypan blue dye exclusion method, and was always greater than 95%. Cells were seeded into 96-well microtiter plates in 100 μL of medium at a density of 5.000–7.500 cells/well and subsequently, the plates were incubated at standard conditions for 24 h to allow the cells to resume exponential growth prior to addition of the compounds. Then, in order to measure the cell population, cells in one plate were fixed *in situ* with TCA followed by SRB staining, as described elsewhere [71]. To determine the compounds activity, each compound dissolved in DMSO was added at 10-fold dilutions (from 100 to 0.01 μM) and incubation continued for an additional period of 48 h. The assay was terminated by addition of cold TCA followed by SRB staining and absorbance measurement at 530 nm, in an EL-311 BIOTEK micro elisa reader (BioTek, Winooski, VT, USA). The dose response parameters such as growth inhibitory activity 50% (GI_{50}) [71], total growth inhibitory activity (TGI) and lethal concentration 50% (LC_{50}) were calculated.

6.2. In vivo assay

6.2.1. Inhibition of the carrageenin-induced oedema [61]

Oedema was induced in the right hind paw of Fisher-344 rats (150–200g) by the intradermal injection of 0.1 mL of 2% carrageenin in water. Both sexes were used. Pregnant females were excluded. Each group consisted of 6–15 animals. The animals, bred in our laboratory, were housed under standard conditions and received a diet of commercial food pellets and water *ad libitum* during the maintenance but they were entirely fasted during the experiment period. Our studies were in accordance with recognized guidelines on animal experimentation.

The tested compounds, 0.01 mmol/kg body weight, were diluted (HCl salt) in water or suspended in water (bases), with few drops of Tween 80 and ground in a mortar before use and were given intraperitoneally simultaneously with the carrageenin injection. The rats were euthanized 3.5 h after carrageenin injection. The difference between the weight of the injected and uninjected paws was calculated for each animal. The change in paw weight was compared with that in control animals (treated with water) and expressed as percent inhibition of the oedema; CPE% values (Table 1). Indomethacin, at 0.01 mmol/kg (47%), was used as

a reference compound. CPE% values are the mean from two different experiments with a standard error of the mean less than 10%.

7. Computational methods, docking simulations

All the molecules were constructed with ChemDraw program [86] and converted in 3D-Structures with the OpenBabel program [87], by using MMFF94 force field.

The X-ray structure of human ALR2 complexed with the inhibitor IDD 594 (PDB code 1US0) [76] was used in our docking calculations, after deletion of the inhibitor IDD 594 from the PDB file, obtained from the Brookhaven Protein Data Bank (PDB) [88]. Although the *in vitro* inhibition assays of our compounds were conducted on rat ALR2, the use of the human ALR2 crystal structure for docking is justified by the facts, that the crystal structure of rat ALR2 is unknown, while the human and rat sequences of this enzyme are characterized by 81% identity and 89% homology [69].

Protein setup was performed using the UCSF Chimera software [89,90]. AnteChamber PYthon Parser interfacE (ACPYPE) tool [91] was employed to generate the topologies of the ligands. ACPYPE tool is written in python to use Antechamber [91,92] to generate topologies for chemical compounds was used for the parametrization of the ligands. Energy minimizations where carried out with the molecular simulation toolkit GROMACS [93] using the AMBER99SB-ILDN force field [94].

Docking calculations were performed with the software Autodock Vina [77,95]. PyRx program [96] was employed to generate the docking input files and to analyze the docking results. The proteins were considered rigid. Performing a blind docking to the ligand IDD 594 and to all developed inhibitors it was found that all the molecules were properly aligned in the active site of 1US0. For all the ligands, the single bonds were considered as active torsional bonds. Docking was carried out with an exhaustiveness value of 64 and a maximum output of 100 binding modes. The conformation obtained for the ligand IDD 594 was almost identical to the crystallized (rmsd 0.090 Å) using the same protocol as above. Simultaneously the results of ligands from protein 1IK3 presented identical conformation in the binding site of 1RRH as they were crystallized in 1IK3.

The final output of the docking procedure is a set of solutions ranked according to the corresponding scoring function values, each defined by the 3D coordinates of its atoms and expressed as a PDB file.

Acknowledgements

The authors would like to thank Drs. C. Hansch, A. Leo and Biobyte Corp. 201 West 4th Street, Suite 204, Claremont, CA 91711, USA for free access to the C-QSAR program. Katsori A.-M. is thankful to “Bodossakis Foundation” and Chatzopoulou M. to the Greek State Scholarship Foundation (IKY) and the Research Committee of Aristotle University of Thessaloniki for financial support.

References

[1] L.M. Espinoza-Fonseca, The benefits of the multi-target approach in drug design and discovery, Bioorg. Med. Chem. 14 (2006) 896–897.
[2] A. Petrelli, S. Giordano, From single- to multi-target drugs in cancer therapy: when aspecificity becomes an advantage, Curr. Med. Chem. 15 (2008) 422–432.
[3] O. Keskin, A. Gursoy, B. Ma, R. Nussinov, Towards drugs targeting multiple proteins in a systems biology approach, Curr. Top. Med. Chem. 7 (2007) 943–951.
[4] F. Sams-Dodd, Target-based drug discovery: is something wrong? Drug Discov. Today 10 (2005) 139–147.
[5] G.R. Zimmermann, J. Lehár, C.T. Keith, Multi-target therapeutics: when the whole is greater than the sum of the parts, Drug Discov. Today 12 (2007) 34–42.
[6] R. Morphy, Z. Rankovic, Designing multiple ligands - medicinal chemistry strategies and challenges, Curr. Pharm. Des. 15 (2009) 587–600.
[7] F. Colotta, P. Allavena, A. Sica, C. Garlanda, A. Mantovani, Cancer-related inflammation, the seventh hallmark of cancer: links to genetic instability, Carcinogenesis 30 (2009) 1073–1081.
[8] A. Mantovani, P. Allavena, A. Sica, F. Balkwill, Cancer-related inflammation, Nature 454 (2008) 436–444.
[9] B.B. Aggarwal, Inflammation, a silent killer in cancer is not so silent!, Curr. Opin. Pharmacol. 9 (2009) 347–350.
[10] M. Cuendet, J.M. Pezzuto, The role of cyclooxygenase and lipoxygenase in cancer chemoprevention, Drug Metabol. Drug Interact. 17 (2000) 109–157.
[11] D.M. Klurfeld, A.W. Bull, Fatty acids and colon cancer in experimental models, Am. J. Clin. Nutr. 66 (1997) 1530S–1538S.
[12] K. Kashfi, S.J. Enna, W. Michael, Anti-inflammatory agents as cancer therapeutics, Advances in Pharmacology. Academic Press, 2009, 31–89.
[13] A.T. Chan, S. Ogino, C.S. Fuchs, Aspirin and the risk of colorectal cancer in relation to the expression of COX-2, N. Engl. J. Med. 356 (2007) 2131–2142.
[14] G.A. Piazza, A.B. Keeton, H.N. Tinsley, J.D. Whitt, B.D. Gary, B. Mathew, R. Singh, W.E. Grizzle, R.C. Reynolds, NSAIDs: old drugs reveal new anticancer targets, Pharmaceuticals 3 (2010) 1652–1667.
[15] W.T. Gunning, P.M. Kramer, V.E. Steele, M.A. Pereira, Chemoprevention by lipoxygenase and leukotriene pathway inhibitors of vinyl carbamate-induced lung tumors in mice, Cancer Res. 62 (2002) 4199–4201.
[16] J. Epstein, I.R. Sanderson, T.T. MacDonald, Curcumin as a therapeutic agent: the evidence from *in vitro*, animal and human studies, Br. J. Nutr. 103 (2010) 1545–1557.
[17] P. Anand, C. Sundaram, S. Jhurani, A.B. Kunnumakkara, B.B. Aggarwal, Curcumin and cancer: an “old-age” disease with an “age-old” solution, Cancer Lett. 267 (2008) 133–164.
[18] E. Sikora, G. Scapagnini, M. Barbagallo, Curcumin, inflammation, ageing and age-related diseases, Immun. Ageing 7 (2010) 1.
[19] M.-H. Teiten, S. Eifes, M. Dicato, M. Diederich, Curcumin—The paradigm of a multi-target natural compound with applications in cancer prevention and treatment, Toxins 2 (2010) 128–162.
[20] B.B. Aggarwal, Y.-J. Surh, S. Shishodia, The molecular targets and therapeutic uses of curcumin in health and disease, Advances in Experimental Medicine and Biology. Springer, US, New York, 2007.
[21] A. Shehzad, F. Wahid, Y.S. Lee, Curcumin in cancer chemoprevention: molecular targets, pharmacokinetics, bioavailability, and clinical trials, Arch. Pharm. (Weinheim) 343 (2010) 489–499.
[22] A. Shehzad, Y.S. Lee, Curcumin: multiple molecular targets mediate multiple pharmacological actions - a review, Drugs Future 35 (2010) 113–119.
[23] B.B. Aggarwal, B. Sung, Pharmacological basis for the role of curcumin in chronic diseases: an age-old spice with modern targets, Trends Pharmacol. Sci. 30 (2009) 85–94.
[24] W.P. Steward, A.J. Gescher, Curcumin in cancer management: recent results of analogue design and clinical studies and desirable future research, Mol. Nutr. Food Res. 52 (2008) 1005–1009.
[25] H. Hatcher, R. Planalp, J. Cho, F. Torti, S. Torti, Curcumin: from ancient medicine to current clinical trials, Cell. Mol. Life Sci. 65 (2008) 1631–1652.
[26] G. Bar-Sela, R. Epelbaum, M. Schaffer, Curcumin as an anti-cancer agent: review of the gap between basic and clinical applications, Curr. Med. Chem. 17 (2010) 190–197.
[27] A. Goel, A.B. Kunnumakkara, B.B. Aggarwal, Curcumin as “Curecumin”: from kitchen to clinic, Biochem. Pharmacol. 75 (2008) 787–809.
[28] P. Anand, A.B. Kunnumakkara, R.A. Newman, B.B. Aggarwal, Bioavailability of curcumin: problems and promises, Mol. Pharm. 4 (2007) 807–818.
[29] E. Burgos-Morón, J.M. Calderón-Montaño, J. Salvador, A. Robles, M. López-Lázaro, The dark side of curcumin, Int. J. Cancer 126 (2010) 1771–1775.
[30] P. Anand, S.G. Thomas, A.B. Kunnumakkara, C. Sundaram, K.B. Harikumar, B. Sung, S.T. Tharakan, K. Misra, I.K. Priyadarsini, K.N. Rajasekharan, B.B. Aggarwal, Biological activities of curcumin and its analogues (congeners) made by man and Mother Nature, Biochem. Pharmacol. 76 (2008) 1590–1611.
[31] D.K. Agrawal, P.K. Mishra, Curcumin and its analogues: potential anticancer agents, Med. Res. Rev. 30 (2010) 818–860.
[32] M.J.C. Rosemond, L. St. John-Williams, T. Yamaguchi, T. Fujishita, J.S. Walsh, Enzymology of a carbonyl reduction clearance pathway for the HIV integrase inhibitor, S-1360: role of human liver cytosolic aldo-keto reductases, Chem. Biol. Interact. 147 (2004) 129–139.
[33] B. Yadav, S. Taurin, R.J. Rosengren, M. Schumacher, M. Diederich, T.J. Somers-Edgar, L. Larsen, Synthesis and cytotoxic potential of heterocyclic cyclohexanone analogues of curcumin, Bioorg. Med. Chem. 18 (2010) 6701–6707.
[34] U. Das, R.K. Sharma, J.R. Dimmock, 1,5-diaryl-3-oxo-1,4-pentadienes: a case for antineoplastics with multiple targets, Curr. Med. Chem. 16 (2009) 2001–2020.
[35] B.K. Adams, E.M. Ferstl, M.C. Davis, M. Herold, S. Kurtkaya, R.F. Camalier, M.G. Hollingshead, G. Kaur, E.A. Sausville, F.R. Rickles, J.P. Snyder, D.C. Liotta, M. Shoji, Synthesis and biological evaluation of novel curcumin analogues as anti-cancer and anti-angiogenesis agents, Bioorg. Med. Chem. 12 (2004) 3871–3883.
[36] P. Lagisetty, D.R. Powell, V. Awasthi, Synthesis and structural determination of 3,5-bis(2-fluorobenzylidene)-4-piperidone analogues of curcumin, J. Mol. Struct. 936 (2009) 23–28.

[37] P. Lagisetty, P. Vilekar, K. Sahoo, S. Anant, V. Awasthi, CLEFMA-An anti-proliferative curcuminoid from structure-activity relationship studies on 3,5-bis(benzylidene)-4-piperidones, Bioorg. Med. Chem. 18 (2010) 6109–6120.

[38] A. Jha, K.M. Duffield, 3,5-Bis(arylmethylene)-4-piperidone derivatives as novel anticancer agents, Indian J. Chem. Sect. B. Org. Chem. Incl. Med. Chem. 45B (2006) 2313–2320.

[39] M.V. Makarov, E.S. Leonova, E.Y. Rybalkina, P. Tongwa, V.N. Khrustalev, T.V. Timofeeva, I.L. Odinets, Synthesis, characterization and structure-activity relationship of novel N-phosphorylated E, E-3,5-bis(thienylidene)piperid-4-ones, Eur. J. Med. Chem. 45 (2010) 992–1000.

[40] U. Das, J. Alcorn, A. Shrivastav, R. Sharma, E. De Clercq, J. Balzarini, J. Dimmock, Design, synthesis and cytotoxic properties of novel 1-[4-(2-alkylaminoethoxy)phenylcarbonyl]-3,5-bis(arylidene)-4-piperidones and related compounds, Eur. J. Med. Chem. 42 (2007) 71–80.

[41] U. Das, M. Kawase, H. Sakagami, A. Ideo, J. Shimada, J. Molnar, Z. Barath, Z. Bata, J. Dimmock, 3-(3,4,5-Trimethoxyphenyl)-1-oxo-2-propene: a novel pharmacophore displaying potent multidrug resistance reversal and selective cytotoxicity, Bioorg. Med. Chem. 15 (2007) 3373–3380.

[42] A.L. Kasinski, Y. Du, S.L. Thomas, J. Zhao, S.Y. Sun, F.R. Khuri, C.Y. Wang, M. Shoji, A. Sun, J.P. Snyder, D. Liotta, H. Fu, Inhibition of IkappaB kinase-nuclear factor-kappaB signaling pathway by 3,5-bis(2-flurobenzylidene) piperidin-4-one (EF24), a novel monoketone analog of curcumin, Mol. Pharmacol. 74 (2008) 654–661.

[43] U. Das, P. Selvakumar, R.K. Sharma, T.A. Haas, J.R. Dimmock, N-Acyl-3,5-bis(arylidene)-4-piperidones and related compounds which stimulate fyn kinase, J. Enzyme Inhib. Med. Chem. 22 (2007) 451–455.

[44] J.R. Dimmock, V.K. Arora, S.L. Wonko, N.W. Hamon, J.W. Quail, Z. Jia, R.C. Warrington, W.D. Fang, J.S. Lee, 3,5-Bisbenzylidene-4-piperidones and related compounds with high activity towards P388 leukemia cells, Drug Des. Deliv. 6 (1990) 183–194.

[45] G. Liang, L. Shao, Y. Wang, C. Zhao, Y. Chu, J. Xiao, Y. Zhao, X. Li, S. Yang, Exploration and synthesis of curcumin analogues with improved structural stability both *in vitro* and *in vivo* as cytotoxic agents, Bioorg. Med. Chem. 17 (2009) 2623–2631.

[46] M.W. Amolins, L.B. Peterson, B.S.J. Blagg, Synthesis and evaluation of electron-rich curcumin analogues, Bioorg. Med. Chem. 17 (2009) 360–367.

[47] a) J.R. Dimmock, M.P. Padmanilayam, R.N. Puthucode, A.J. Nazarali, N.L. Motaganahalli, G.A. Zello, J.W. Quail, E.O. Oloo, H.-B. Kraatz, J.S. Prisciak, T.M. Allen, C.L. Santos, J. Balzarini, E. De Clercq, E.K. Manavathu, A conformational and structure-activity relationship study of cytotoxic 3,5-bis(arylidene)-4-piperidones and related N-acryloyl analogues, J. Med. Chem. 44 (2001) 586–593;
b) J.R. Dimmock, V.K. Arora, M. Chen, T.M. Allen, G.Y. Kao, Cytotoxic evaluation of some N-acyl and N-acyloxy analogs of 3,5-bis(arylidene)-4-piperidones, Drug Des. Discov. 12 (1994) 19–28.

[48] H.I. El-Subbagh, S.M. Abu-Zaid, M.A. Mahran, F.A. Badria, A.M. Al-Obaid, Synthesis and biological evaluation of certain alpha, beta-unsaturated ketones and their corresponding fused pyridines as antiviral and cytotoxic agents, J. Med. Chem. 43 (2000) 2915–2921.

[49] D.V. Jovanovic, J.C. Fernandes, J. Martel-Pelletier, F.C. Jolicoeur, P. Reboul, S. Laufer, S. Tries, J.P. Pelletier, *In vivo* dual inhibition of cyclooxygenase and lipoxygenase by ML-3000 reduces the progression of experimental osteoarthritis: suppression of collagenase 1 and interleukin-1beta synthesis, Arthritis Rheum. 44 (2001) 2320–2330.

[50] C. Menna, F. Olivieri, A. Catalano, A. Procopio, Lipoxygenase inhibitors for cancer prevention: promises and risks, Curr. Pharm. Des. 16 (2010) 725–733.

[51] L.G. Melstrom, D.J. Bentrem, M.R. Salabat, T.J. Kennedy, X.Z. Ding, M. Strouch, S.M. Rao, R.C. Witt, C.A. Ternent, M.S. Talamonti, R.H. Bell, T.A. Adrian, Overexpression of 5-lipoxygenase in colon polyps and cancer and the effect of 5-LOX inhibitors *in vitro* and in a murine model, Clin. Cancer Res. 14 (2008) 6525–6530.

[52] L.T. Soumaoro, S. Iida, H. Uetake, M. Ishiguro, Y. Takagi, T. Higuchi, M. Yasuno, M. Enomoto, K. Sugihara, Expression of 5-lipoxygenase in human colorectal cancer, World J. Gastroenterol. 12 (2006) 6355–6360.

[53] J. Clària, M. Romano, Pharmacological intervention of cyclooxygenase-2 and 5-lipoxygenase pathways. Impact on inflammation and cancer, Curr. Pharm. Des. 11 (2005) 3431–3447.

[54] X.Z. Ding, R. Hennig, T.E. Adrian, Lipoxygenase and cyclooxygenase metabolism: new insights in treatment and chemoprevention of pancreatic cancer, Mol. Cancer 2 (2003) 10.

[55] E. Pontiki, D. Hadjipavlou-Litina, G. Geromichalos, A. Papageorgiou, Anticancer activity and quantitative-structure activity relationship (QSAR) studies of a series of antioxidant/anti-inflammatory aryl-acetic and hydroxamic acids, Chem. Biol. Drug Des. 74 (2009) 266–275.

[56] C.V. Rao, Regulation of COX and LOX by curcumin. in: B.B. Aggarwal, Y.-J. Surh, S. Shishodia (Eds.), The Molecular Targets and Therapeutic Uses of Curcumin in Health and Disease. Springer, US, 2007, pp. 213–226.

[57] E. Skrzypczak-Jankun, N.P. McCabe, S.H. Selman, J. Jankun, Curcumin inhibits lipoxygenase by binding to its central cavity: theoretical and X-ray evidence, Int. J. Mol. Med. 6 (2000) 521–526.

[58] J. Hong, M. Bose, J. Ju, J.-H. Ryu, X. Chen, S. Sang, M.-J. Lee, C.S. Yang, Modulation of arachidonic acid metabolism by curcumin and related β-diketone derivatives: effects on cytosolic phospholipase A2, cyclooxygenases and 5-lipoxygenase, Carcinogenesis 25 (2004) 1671–1679.

[59] C. Pergola, O. Werz, 5-Lipoxygenase inhibitors: a review of recent developments and patents, Expert Opin. Ther. Pat. 20 (2010) 355–375.

[60] I.B. Taraporewala, J.M. Kauffman, Synthesis and structure-activity relationships of anti-inflammatory 9,10-dihydro-9-oxo-2-acridine-alkanoic acids and 4-(2-carboxyphenyl)aminobenzenealkanoic acids, J. Pharm. Sci. 79 (1990) 173–178.

[61] E. Pontiki, D. Hadjipavlou-Litina, Antioxidant and anti-inflammatory activity of aryl-acetic and hydroxamic acids as novel lipoxygenase inhibitors, Med. Chem. 2 (2006) 251–264.

[62] E. Pontiki, D. Hadjipavlou-Litina, Lipoxygenase inhibitors: a comparative QSAR study review and evaluation of new QSARs, Med. Res. Rev. 28 (2008) 39–117.

[63] K. Muller, 5-Lipoxygenase and 12-lipoxygenase: attractive targets for the development of novel antipsoriatic drugs, Arch. Pharm. (Weinheim) 327 (1994) 3–19.

[64] P. Alexiou, K. Pegklidou, M. Chatzopoulou, I. Nicolaou, V.J. Demopoulos, Aldose reductase enzyme and its implication to major health problems of the 21(st) century, Curr. Med. Chem. 16 (2009) 734–752.

[65] K.V. Ramana, S.K. Srivastava, Aldose reductase: a novel therapeutic target for inflammatory pathologies, Int. J. Biochem. Cell Biol. 42 (2010) 17–20.

[66] N. Halder, S. Joshi, S.K. Gupta, Lens aldose reductase inhibiting potential of some indigenous plants, J. Ethnopharmacol. 86 (2003) 113–116.

[67] P. Muthenna, P. Suryanarayana, K.G. Shravan, J.M. Petrash, G.B. Reddy, Inhibition of aldose reductase by dietary antioxidant curcumin: mechanism of inhibition, specificity and significance, FEBS Lett. 583 (2009) 3637–3642.

[68] Z.-Y. Du, Y.-D. Bao, Z. Liu, W. Qiao, L. Ma, Z.-S. Huang, L.-Q. Gu, A.S.C. Chan, Curcumin analogs as potent aldose reductase inhibitors, Arch. Pharm. (Weinheim) 339 (2006) 123–128.

[69] T. Gui, T. Tanimoto, Y. Kokai, C. Nishimura, Presence of a closely related subgroup in the aldo-ketoreductase family of the mouse, Eur. J. Biochem. 227 (1995) 448–453.

[70] A. Del Corso, L. Costantino, G. Rastelli, F. Buono, U. Mura, Aldose reductase does catalyse the reduction of glyceraldehyde through a stoichiometric oxidation of NADPH, Exp. Eye Res. 71 (2000) 515–521.

[71] K. Dimas, S. Hatziantoniou, S. Tseleni, H. Khan, A. Georgopoulos, K. Alevizopoulos, J. Wyche, P. Pantazis, C. Demetzos, Sclareol induces apoptosis in human HCT116 colon cancer cells in vitro and suppression of HCT116 tumor growth in immunodeficient mice, Apoptosis 12 (2007) 685–694.

[72] BioByte Corporation, C-QSAR database 201 West 4th Str., Suite 204, Claremont, California 91711, USA.

[73] C. Kontogiorgis, K. Litinas, A. Makri, D. Nicolaides, A. Vronteli, D. Hadjipavlou-Litina, E. Pontiki, A. Siohou, Synthesis and biological evaluation of novel angular fused pyrrolocoumarins, J. Enzyme Inhib. Med. Chem. 23 (2008) 43–49.

[74] P. Brooks, R. Day, Nonsteroidal antiinflammatory drugs–differences and similarities, N. Engl. J. Med. 324 (1991) 1716–1725.

[75] V.R. Shanbhag, A.M. Crider, R. Gokhale, A. Harpalani, R.M. Dick, Ester and amide prodrugs of ibuprofen and naproxen: synthesis, anti-inflammatory activity, and gastrointestinal toxicity, J. Pharm. Sci. 81 (1992) 149–154.

[76] E.I. Howard, R. Sanishvili, R.E. Cachau, A. Mitschler, B. Chevrier, P. Barth, V. Lamour, M. Van Zandt, E. Sibley, C. Bon, D. Moras, T.R. Schneider, A. Joachimiak, A. Podjarny, Ultrahigh resolution drug design I: details of interactions in human aldose reductase–inhibitor complex at 0.66 Å, Proteins 55 (2004) 792–804.

[77] O. Trott, A.J. Olson, AutoDock Vina: improving the speed and accuracy of docking with a new scoring function, efficient optimization, and multithreading, J. Comput. Chem. 31 (2010) 455–461.

[78] M. Chatzopoulou, E. Mamadou, M. Juskova, C. Koukoulitsa, I. Nicolaou, M. Stefek, V.J. Demopoulos, Structure activity relations on [1-(3,5-difluoro-4-hydroxyphenyl)-1H-pyrrol-3-yl]phenylmethanone. The effect of methoxy substitution on aldose reductase inhibitory activity and selectivity, Bioorg. Med. Chem. 19 (2011) 1426–1433.

[79] K.M. Bohren, C.E. Grimshaw, C.J. Lai, D.H. Harrison, D. Ringe, G.A. Petsko, K.H. Gabbay, Tyrosine-48 is the proton donor and histidine-110 directs substrate stereochemical selectivity in the reduction reaction of human aldose reductase: enzyme kinetics and crystal structure of the Y48H mutant enzyme, Biochemistry 33 (1994) 2021–2032.

[80] C.E. Grimshaw, K.M. Bohren, C.-J. Lai, K.H. Gabbay, Human aldose reductase: pK of tyrosine 48 reveals the preferred ionization state for catalysis and inhibition, Biochemistry 34 (1995) 14374–14384.

[81] A. Podjarny, R.E. Cachau, T. Schneider, M. Van Zandt, A. Joachimiak, Subatomic and atomic crystallographic studies of aldose reductase: implications for inhibitor binding, Cell. Mol. Life Sci. 61 (2004) 763–773.

[82] W. Minor, J. Steczko, B. Stec, Z. Otwinowski, J.T. Bolin, R. Walter, B. Axelrod, Crystal structure of soybean lipoxygenase L-1 at 1.4 Å resolution, Biochemistry 35 (1996) 10687–10701.

[83] E. Pontiki, D. Hadjipavlou-Litina, K. Litinas, O. Nicolotti, A. Carotti, Design, synthesis and pharmacobiological evaluation of novel acrylic acid derivatives acting as lipoxygenase and cyclooxygenase-1 inhibitors with antioxidant and anti-inflammatory activities, Eur. J. Med. Chem. 46 (2011) 191–200.

[84] H. Berman, K. Henrick, H. Nakamura, Announcing the worldwide Protein Data Bank, Nat. Struct. Mol. Biol. 10 (2003) 980.

[85] J.R. Dimmock, U. Das, Antineoplastic Compounds, WO/2007/059613 (2007).

[86] CambridgeSoft, USA, ChemDraw Ultra© v.12 (1986–2009).http://www.cambridgesoft.com/software/ChemDraw/.
[87] OpenBabel© v.2.2.3 (2006).http://sourceforge.net/projects/openbabel/.
[88] RCSB Protein Data Bank, operated by the Research Collaboratory for Structural Bioinformatics. www.pdb.org/.
[89] http://www.cgl.ucsf.edu/chimera
[90] E.F. Pettersen, T.D. Goddard, C.C. Huang, G.S. Couch, D.M. Greenblatt, E.C. Meng, T.E. Ferrin, UCSF Chimera–A visualization system for exploratory research and analysis, J. Comput. Chem. 25 (2004) 1605–1612.
[91] J. Wang, R.M. Wolf, J.W. Caldwell, P.A. Kollman, D.A. Case, Development and testing of a general amber force field, J. Comput. Chem. 25 (2004) 1157–1174.
[92] J. Wang, W. Wang, P.A. Kollman, D.A. Case, Automatic atom type and bond type perception in molecular mechanical calculations, J. Mol. Graph. Model. 25 (2006) 247–260.
[93] B. Hess, C. Kutzner, D. van der Spoel, E. Lindahl, GROMACS 4: algorithms for highly efficient, load-balanced, and scalable molecular simulation, J. Chem. Theory Comput. 4 (2008) 435–447.
[94] K. Lindorff-Larsen, S. Piana, K. Palmo, P. Maragakis, J.L. Klepeis, R.O. Dror, D.E. Shaw, Improved side-chain torsion potentials for the Amber ff99SB protein force field, Proteins 78 (2010) 1950–1958.
[95] Autodock Vina v. 1.1.1. Copyright© 1989–2010, The Scripps Research Institute.
[96] Sargis Pallakyan, PyRx-Python Prescription, v.0.5. The Scripps Research Institute, 2008–2010.http://pyrx.scripps.edu/.